Pairing interaction near a nematic quantum critical point of a three-band CuO_2 model

T. A. Maier
Computer Science and Mathematics Division and Center for Nanophase Materials Sciences, Oak Ridge National Laboratory, Oak Ridge, Tennessee 37831-6494, USA

D. J. Scalapino
Department of Physics, University of California, Santa Barbara, California 93106-9530, USA

(Received 20 May 2014; revised manuscript received 2 October 2014; published 21 November 2014)

Here we calculate the pairing interaction and the k dependence of the gap function associated with the nematic charge fluctuations of a CuO_2 model. We find that the nematic pairing interaction is attractive for small momentum transfer and that it gives rise to d-wave pairing. As the doping p approaches a quantum critical point, the strength of this pairing increases and higher d-wave harmonics contribute to the k dependence of the superconducting gap function, reflecting the longer range nature of the nematic fluctuations.

DOI: 10.1103/PhysRevB.90.174510 PACS number(s): 74.20.Mn, 74.62.Bf, 74.62.Dh, 74.72.−h

The importance of a nematic phase and the possible existence of a nematic quantum critical point (QCP) just beyond the optimal doping of the cuprate superconductors was raised in an article by Kivelson *et al.* [1]. There are now a variety of experiments [2–7], which find short-range biaxial charge order in the pseudogap region of the T-p (p = holes/Cu) phase diagram of the cuprate superconductors. Ultrasonic measurements [8] of the elastic moduli of $YBaCuO_{6+\delta}$ crystals provide thermodynamic evidence of a distinct phase boundary $T^*(p)$ below which the system is in a pseudogap phase. Magnetoresistance measurements of the electron effective mass m^* by Ramshaw *et al.* [9] report an increase in m^* as the doping p approaches a critical doping $p_c = 0.18$ where $T^*(p_c)$ goes to zero. They also find that the magnetic field needed to suppress superconductivity peaks as p approaches p_c, clearly implicating the pseudogap quantum critical fluctuations in the superconducting pairing. There have also been a number of theoretical ideas regarding nematic and spin-charge order and in particular the nature of the pseudogap and its role in superconductivity [10–12]. Oganesyan *et al.* [13] discussed the breakdown of Fermi-liquid theory at a nematic quantum critical point. Metlitski *et al.* [14–16] have argued that near the onset of spin-density wave (SDW) order there is an instability to an Ising nematic charge ordered phase and discussed how nematic critical point fluctuations can mediate pairing. Nie *et al.* [17] have noted that a number of experimental observations associated with the pseudogap can be understood if the phase is a nematic remnant of stripe order.

Here we examine this problem phenomenologically using the framework of a three-band Hubbard model for a CuO_2 plane [18,19] to parametrize the nematic fluctuations. Early studies of this model [20] found that interband charge-transfer excitations could promote s-wave superconductivity. Recent work by Fischer and Kim [21] and Bulut *et al.* [22] has shown that this model exhibits nematic instabilities and studied its phase diagram. We are interested in determining the strength of the d-wave pairing associated with nematic fluctuations and the k dependence of the gap function as the doping p approaches p_c. We will find the following: (1) Nematic charge fluctuations can work in parallel with a primary d-wave pairing interaction such as antiferromagnetic spin fluctuations; (2) the attractive pairing nematic fluctuations involve small momentum transfers $|k - k'|$ for which the gap $\Delta(k)$ and $\Delta(k')$ have the same sign; (3) as the doping p approaches the QCP, the strength of the pairing gets larger and the increasing range of the interaction is reflected in higher d-wave harmonic structure in the k-dependence of the gap.

In the three-band Hubbard model [18,19] for the CuO_2 layer, the single-particle electron creation operators carry an orbital index ℓ. This index $\ell = 1$, 2, or 3 and denotes respectively the $d_{x^2-y^2}$ orbit of the Cu, the p_x orbit of the O_x oxygen and the p_y orbit of the O_y oxygen in the unit cell. The Hamiltonian is

$$H = H_0 + V \tag{1}$$

with

$$H_0 = \sum_{k,\ell_1,\ell_2,\sigma} \big(\varepsilon_{\ell_1\ell_2}(k) - \mu\big) c^\dagger_{\ell_1\sigma}(k) c_{\ell_2\sigma}(k). \tag{2}$$

For the hopping parameters shown in Fig. 1(a)

$$\begin{aligned}\varepsilon_{\ell_1\ell_2}(k) = {} & \varepsilon_d\, \delta_{\ell_1,1}\delta_{\ell_2,1} + \varepsilon_p \left[\delta_{\ell_1,2}\delta_{\ell_2,2} + \delta_{\ell_1,3}\delta_{\ell_2,3}\right] \\ & + 2t_{pd} \sin(k_x/2) \left[\delta_{\ell_1,1}\delta_{\ell_2,2} + \delta_{\ell_1,2}\delta_{\ell_2,1}\right] \\ & - 2t_{pd} \sin(k_y/2) \left[\delta_{\ell_1,1}\delta_{\ell_2,3} + \delta_{\ell_1,3}\delta_{\ell_2,1}\right] \\ & - 4t_{pp} \sin(k_x/2) \sin(k_y/2) \left[\delta_{\ell_1,2}\delta_{\ell_2,3} + \delta_{\ell_1,3}\delta_{\ell_2,2}\right].\end{aligned} \tag{3}$$

Diagonalization of H_0 gives three bands ν with energy dispersion $E_\nu(k)$. V contains the Coulomb interactions indicated in Fig. 1(a) and is given by

$$V = \sum_{\ell_1\ell_2} V_{\ell_1\ell_2}(q) n_{\ell_1}(q) n_{\ell_2}(-q) \tag{4}$$

with

$$n_\ell(q) = \sum_{k,\sigma} c^\dagger_{\ell\sigma}(k+q) c_{\ell\sigma}(k) \tag{5}$$

and

$$\begin{aligned}V_{\ell_1\ell_2}(q) = {} & U_d\big[\delta_{\ell_1,1}\delta_{\ell_2,1}\big] + U_p\big[\delta_{\ell_1,2}\delta_{\ell_2,2} + \delta_{\ell_1,3}\delta_{\ell_2,3}\big] \\ & + 2V_{pd} \cos(q_x/2)\big[\delta_{\ell_1,1}\delta_{\ell_2,2} + \delta_{\ell_1,2}\delta_{\ell_2,1}\big] \\ & + 2V_{pd} \cos(q_y/2)\big[\delta_{\ell_1,1}\delta_{\ell_2,3} + \delta_{\ell_1,3}\delta_{\ell_2,1}\big] \\ & + 4V_{pp} \cos(q_x/2) \cos(q_y/2)\big[\delta_{\ell_1,2}\delta_{\ell_2,3} + \delta_{\ell_1,3}\delta_{\ell_2,2}\big].\end{aligned} \tag{6}$$

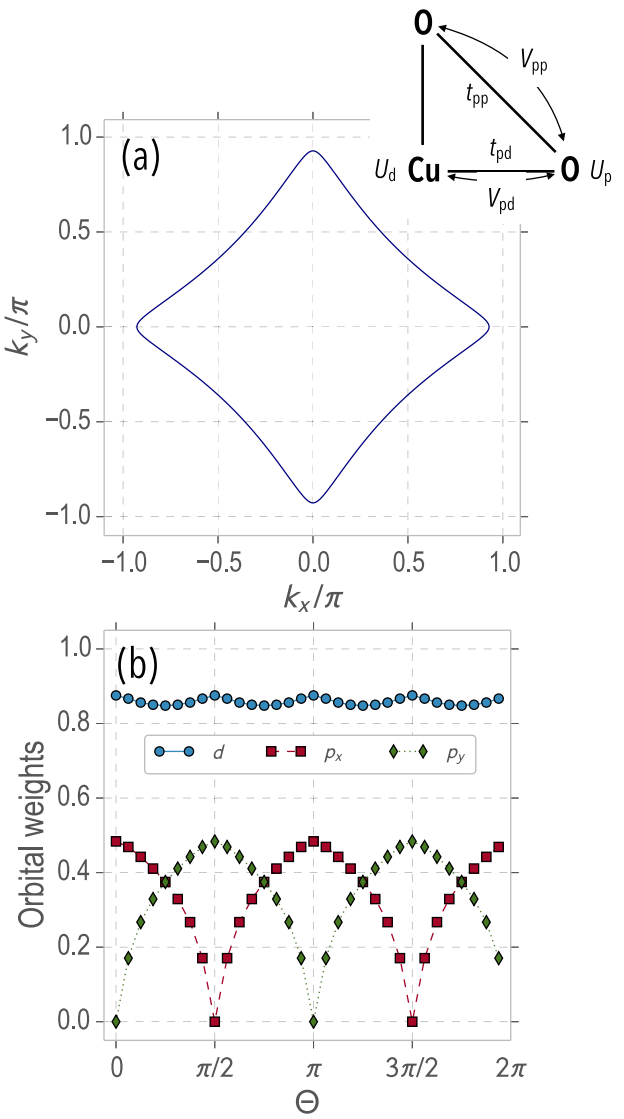

FIG. 1. (Color online) (a) The Fermi surface for $t_{pd} = 1.0, t_{pp} = 0.5$ at a hole doping $p = 0.20$. The inset shows the hopping and Coulomb interactions parameters. (b) The orbital weights $|a^l_\nu(k)|$ on the Fermi surface with the angle Θ measured from $k = (\pi,0)$.

The effective interaction in the charge channel consists of the direct and the exchange terms

$$V^c_{\ell_1\ell_2\ell_3\ell_4}(k,k',q) = -\delta_{\ell_1\ell_3}\delta_{\ell_2\ell_4}V_{\ell_1\ell_2}(k-k') + \delta_{\ell_1\ell_2}\delta_{\ell_3\ell_4}2V_{\ell_1\ell_3}(q). \quad (7)$$

Within an RPA approximation the charge vertex Γ^c is obtained as the solution of the particle-hole t matrix which sums multiple V^c scatterings. This integral equation can be simplified by writing the interaction in a separable form [23],

$$V_{\ell_1\ell_2}(k-k') = \sum_{ij} g^i_{\ell_1\ell_2}(k)\tilde{V}^{ij}_X g^j_{\ell_1\ell_2}(k'),$$
$$V_{\ell_1\ell_2}(q) = \sum_{ij} g^i_{\ell_1\ell_1}\tilde{V}^{ij}_D(q) g^j_{\ell_2\ell_2}. \quad (8)$$

The functions $g^i_{\ell_1\ell_2}(k)$ form a 19-dimensional basis. This basis along with the 19×19 exchange $\tilde{V}_X$ and direct $\tilde{V}_D$ interaction matrices are given in Appendix A of Bulut *et al.* [22].

The charge vertex is then given by

$$\Gamma^c_{\ell_1\ell_2\ell_3\ell_4}(k,k',q) = \sum_{ij} g^i_{\ell_1\ell_2}(k)\tilde{\Gamma}^{ij}_c(q) g^j_{\ell_3\ell_4}(k') \quad (9)$$

with

$$\tilde{\Gamma}_c(q) = [1 + \tilde{V}_c(q)\tilde{\chi}_0(q)]^{-1}\tilde{V}_c(q). \quad (10)$$

Here $\tilde{V}_c(q) = 2\tilde{V}_D(q) - \tilde{V}_X(q)$ and

$$\tilde{\chi}^{ij}_0(q) = -\frac{1}{N}\sum_{k,\mu,\nu}\sum_{\ell_1,\ell_2,\ell_3,\ell_4} g^i_{\ell_4\ell_3}(k) M^{\ell_1\ell_2\ell_3\ell_4}_{\mu\nu}(k,q) g^j_{\ell_2\ell_1}(k) \times \frac{f(E_\nu(k+q)) - f(E_\mu(k))}{E_\nu(k+q) - E_\mu(k)} \quad (11)$$

with $M^{\ell_1\ell_2\ell_3\ell_4}_{\mu\nu}(k,q) = a^{\ell_4}_\mu(k) a^{\ell_2^*}_\mu(k) a^{\ell_1}_\nu(k+q) a^{\ell_3^*}_\nu(k+q)$, where $a^\ell_\nu(k) = \langle c_\ell | \nu k\rangle$ are orbital-band matrix-elements shown in Fig. 1(b). Within an RPA approximation, the charge susceptibility matrix

$$\chi_{\ell_1\ell_2}(q) = \int_0^\beta d\tau \left\langle \mathcal{T} n_{\ell_1}(q,\tau) n_{\ell_2}(-q,0)\right\rangle \quad (12)$$

is obtained from $\tilde{\Gamma}_c$ as [22]

$$\chi_{\ell_1\ell_2}(q) = \chi^0_{\ell_1\ell_2}(q) - \sum_{ij} A^i_{\ell_1\ell_1}(q)\tilde{\Gamma}^{ij}_c(q) A^j_{\ell_2\ell_2}(q) \quad (13)$$

with

$$\chi^0_{\ell_1\ell_2}(q) = -\frac{1}{N}\sum_{k,\mu,\nu} M^{\ell_1\ell_1\ell_2\ell_2}_{\mu\nu}(k,q)\frac{f(E_\nu(k+q)) - f(E_\mu(k))}{E_\nu(k+q) - E_\mu(k)},$$

$$A^i_{\ell_3\ell_4}(q) = \frac{1}{N}\sum_{k,\mu,\nu}\sum_{\ell_1,\ell_2} M^{\ell_1\ell_2\ell_3\ell_4}_{\mu\nu}(k,q) g^i_{\ell_1\ell_2}(k) \times \frac{f(E_\nu(k+q)) - f(E_\mu(k))}{E_\nu(k+q) - E_\mu(k)}. \quad (14)$$

The nematic susceptibility is given by the d-wave projection of the charge susceptibility

$$\chi_N(q) = \chi_{xx}(q) + \chi_{yy}(q) - \chi_{xy}(q) - \chi_{yx}(q), \quad (15)$$

with $\chi_{\ell_1\ell_2}(q)$ given by Eq. (13). The charge vertex enters the pairing channel as illustrated in the inset of Fig. 3. A measure of the pairing strength and the k-dependent structure of the gap function [24] is given by the leading eigenvalue and eigenfunction of

$$-\oint \frac{dk'_\parallel}{2\pi v_F(k'_\parallel)}\Gamma_c(k,k')\phi_\alpha(k') = \lambda_\alpha\phi_\alpha(k) \quad (16)$$

with

$$\Gamma_c(k,k') = \sum_{\ell_1,\ell_2,\ell_3,\ell_4} a^{\ell_1^*}_\nu(k) a^{\ell_4^*}_\nu(-k)\Gamma^c_{\ell_1\ell_2\ell_3\ell_4}(k',-k,k-k') \times a^{\ell_2}_\mu(k') a^{\ell_3}_\mu(-k'). \quad (17)$$

Here the $k_\parallel$ integral in Eq. (16) is over the Fermi surface, ν is the band index at the Fermi energy, and $v_F(k_\parallel)$ is the Fermi velocity.

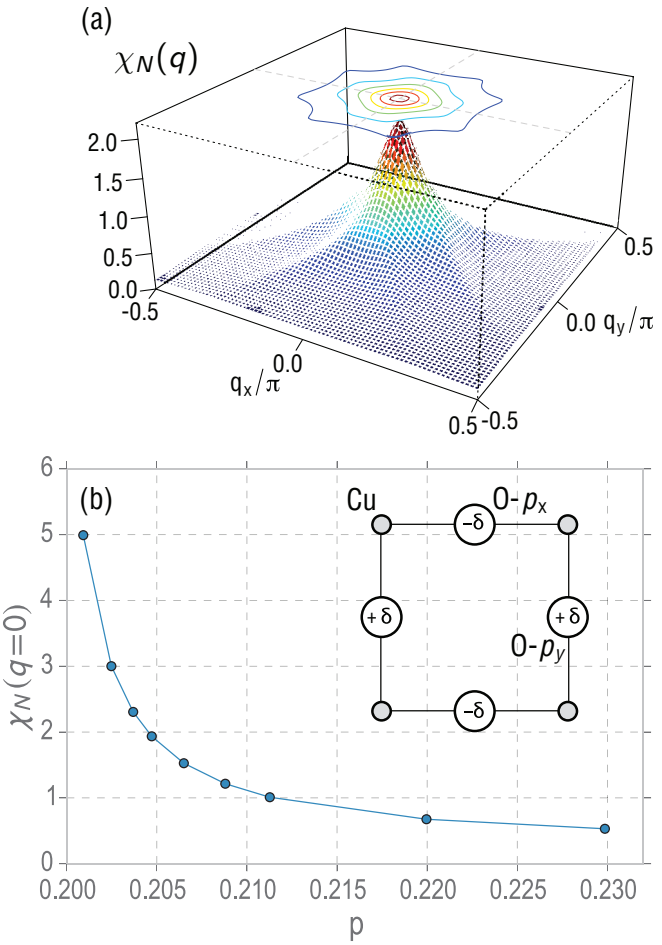

FIG. 2. (Color online) The RPA nematic charge susceptibility $\chi_N(q)$ vs q for $p = 0.205$. (b) $\chi_N(q = 0)$ vs p. The inset illustrates the nematic mode charge fluctuation on the oxygens.

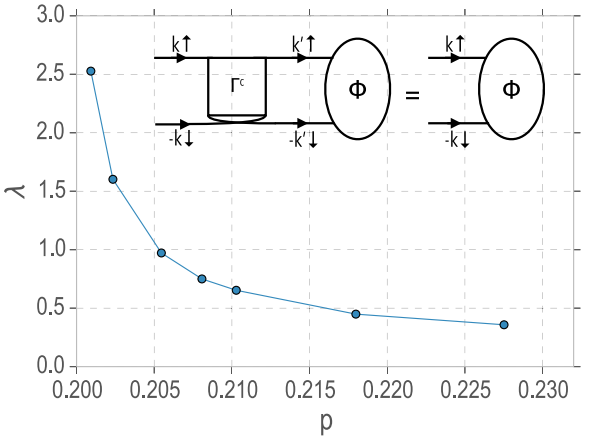

FIG. 3. (Color online) The d-wave pairing strength λ_d associated with the exchange of charge fluctuations vs the hole doping p. The inset shows a diagrammatic representation of the contribution of the charge vertex Γ_c to the gap equation.

In the following we will measure energy in units of t_{pd} and set $t_{pp} = 0.5$, $\varepsilon_d - \varepsilon_p = 2.5$, $U_d = 9$, $U_p = 3$, $V_{pd} = 1$, and $V_{pp} = 2$. For these parameters there is a phase transition to a commensurate $q = 0$ nematic phase when the doping decreases below a critical doping $p_c \approx 0.20$ [22]. The Fermi surface for this doping is shown in Fig. 1(a). Here we examine the contribution of the nematic fluctuations to the pairing which arises from the charge channel [25]. In this RPA formulation we assume that the energy scale of the nematic fluctuations which drive the pairing is larger than T_c and evaluate the charge pairing vertex Γ_c and the nematic susceptibility χ_N in the $T \to 0$ limit. This procedure of course breaks down in the critical regime when p is close to p_c. Pairing near an Ising-nematic QCP has been discussed in Ref. [16].

The nematic (d-wave) charge susceptibility $\chi_N(q)$ evaluated from Eq. (15) is shown in Fig. 2(a) for a doping $p = 0.205$. As discussed by Bulut *et al.* [22], depending upon the model parameters, commensurate $q = (0,0)$ (nematic), diagonal $q = (q_0,q_0)$ (smecticlike), or Cu-O-Cu bond aligned $q = (q_0,0)$, $(0,q_0)$ (smecticlike) phases can occur. In all these cases the charge transfer is dominantly between the $O - p_x$ and $O - p_y$ oxygen orbitals, as illustrated in the inset of Fig. 2(b). This same intraunit cell breaking of the point-group symmetry of the CuO_2 lattice was found in a strong-coupling limit of the three-band Emery model [26], while the $q = (q_0,0)$ phase is observed in the cuprates [5]. For the interaction parameters we have used, the susceptibility diverges at $p_c \approx 0.20$ where there is a commensurate $q = (0,0)$ quantum critical point. As shown in Fig. 2(b), the nematic susceptibility $\chi_N(q = 0)$ rises rapidly as p approaches p_c. For a fixed value of $p - p_c$, the strength of the nematic fluctuations depend on the oxygen-oxygen interaction V_{pp} and increase as V_{pp} increases.

We turn next to the pairing channel. The nematic fluctuations with $q = 0$ give rise to an attractive pairing interaction for small momentum transfer $k - k'$. For large momentum transfer, the pairing interaction is repulsive because of the leading order $V^c(k,k',q)$ contribution to $\Gamma^c(k,k',q)$ [see Eq. (10)]. We find that this structure of the pairing interaction in Eq. (16) gives rise to a leading d-wave (see Fig. 4) and a subleading extended s-wave (not shown) eigenfunction $\phi_\alpha(k)$ with nearly degenerate eigenvalues. As shown in Fig. 3, the eigenvalue λ_d which is a measure of the d-wave pairing strength increases as p approaches p_c. The nematic fluctuations are attractive and contribute positively to the d-wave pairing because they involve small momentum transfers. At a fixed $p - p_c$ value, λ_d increases when V_{pp} is increased and the nematic fluctuations increase in strength. In addition, in this RPA treatment, λ_d has a strong dependence on the Coulomb interaction V_{pd} between the Cu and the O. While the strength of the nematic fluctuations primarily depend upon p and V_{pp}, their contribution to the pairing vertex $\Gamma_c(k,k')$ depends on V_{pd}. This is because V_{pd} provides a coupling of the $O - p_x$ and the $O - p_y$ charge fluctuations to Γ^c_{dddd} which as seen in Eq. (17) contributes to $\Gamma^c(k,k')$ through four d orbital weight factors. In the absence of the V_{pd} coupling, a coupling of the nematic oxygen charge fluctuations to the d-wave pairing channel involves the product of four p orbital weight factors, which, as seen from Fig. 1(b), is significantly smaller than the product of four d-orbital weight factors. Here it is important to remember that the RPA is a weak-coupling theory and in strong coupling a large U_d splits the band at the Fermi energy into a lower and an upper Hubbard band. Hole doping then moves the chemical potential

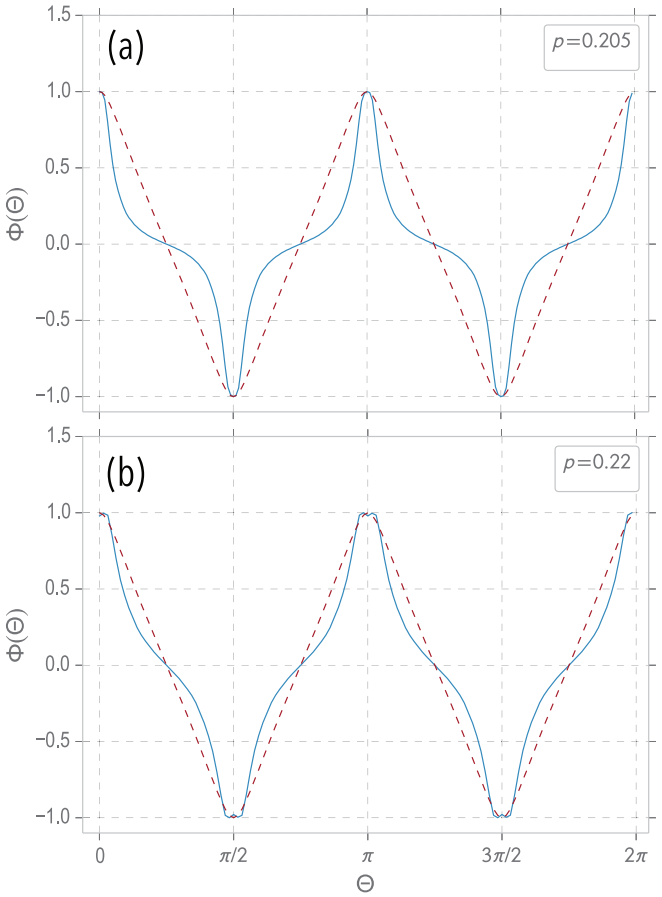

FIG. 4. (Color online) The gap function $\phi_d(k)$ (solid) vs θ for k on the Fermi surface normalized to its value at $\theta = 0$. The dashed curve is $\cos k_x - \cos k_y$. (a) $p = 0.205$ and (b) $p = 0.22$.

into the band that has predominantly p character and in this case, V_{pd} will play a less important role in the coupling to the nematic fluctuations.

The gap functions $\phi_d(k)$ for dopings $p = 0.205$ and 0.22 are shown as the solid curves in Figs. 4(a) and 4(b). The deviation of $\phi_d(k)$ from the $(\cos k_x - \cos k_y)$ form shown as the dashed curves implies the presence of additional higher-order d-wave harmonics. As one knows, the pairing interaction associated with short-range antiferromagnetic spin fluctuations primarily involves near-neighbor Cu sites and leads to the familiar $(\cos k_x - \cos k_y)$ dependence of $\phi_d(k)$. However, as seen in the plot of $\chi_N(q)$, Fig. 2(a), the nematic fluctuations close to the QCP are rather narrow leading to a longer range interaction and increasing the weight of higher harmonics in $\phi_d(k)$. This becomes particularly apparent in the structure of $\phi_d(k)$ as p approaches p_c. As noted, the yttrium based cuprates have Cu-O-Cu bond aligned incommensurate $q^* = (q_0,0)$ or $(0,q_0)$ charge fluctuations. In this case, there will be eight regions associated with the Fermi-surface points connected by q^* where $\phi_d(k)$ will exhibit additional structure. Again, this structure will narrow and peak as p approaches p_c.

Using an RPA approximation for a three-band model of CuO_2 we have shown that nematic charge fluctuations can contribute to the d-wave pairing interaction and that the strength of this pairing increases as the doping p approaches the nematic QCP. The pairing interaction mediated by the nematic fluctuations is "attractive" for frequencies below a characteristic fluctuation scale and involves small momentum transfers. Thus it predominantly scatters pairs between $(k,-k)$ and $(k',-k')$ states on the Fermi surface where the gap has the same sign. Because of the large on-site Cu Coulomb interaction, the pairing occurs in the d-wave channel. The narrow linewidth associated with the nematic pairing interaction close to the QCP leads to higher d-wave harmonics in the k dependence of the gap, reflecting the longer range nature of the nematic pairing interaction. The nematic fluctuations can work in tandem with the "repulsive" large momentum transfer spin fluctuation interaction so that both the charge and spin channels contribute to the d-wave pairing strength.

Note added. As this paper was being completed, we became aware of complementary work by S. Lederer, Y. Schattner, E. Berg, and S. A. Kivelson who studied the problem of enhancement of superconductivity near a nematic quantum critical point. Their conclusions are similar to ours [27].

We want to thank W. Hardy, S. Kivelson and M. Metlitski for useful discussions and acknowledge the support of the Center for Nanophase Materials Sciences, which is sponsored at Oak Ridge National Laboratory by the Scientific User Facilities Division, Office of Basic Energy Sciences, US Department of Energy.

[1] S. A. Kivelson, E. Fradkin, and V. J. Emery, Nature (London) **393**, 550 (1998).
[2] T. Wu, H. Mayaffre, S. Krmer, M. Horvati, C. Berthier, W. N. Hardy, R. Liang, D. A. Bonn, and M.-H. Julien, Nature (London) **477**, 191 (2011).
[3] K. Fujita, M. H. Hamidian, S. D. Edkins, Chung Koo Kim, Y. Kohsaka, M. Azuma, M. Takano, H. Takagi, H. Eisaki, S. Uchida, A. Allais, M. J. Lawler, E.-A. Kim, Subir Sachdev, and J. C. Séamus Davis, Proc. Nat. Acad. Sci. **111**, E3026 (2014).
[4] D. LeBoeuf, S. Krämer, W. N. Hardy, Ruixing Liang, D. A. Bonn, and C. Proust, Nat. Phys. **9**, 79 (2013).
[5] E. Blackburn, J. Chang, M. Hücker, A. T. Holmes, N. B. Christensen, Ruixing Liang, D. A. Bonn, W. N. Hardy, U. Rütt, O. Gutowski, M. v. Zimmermann, E. M. Forgan, and S. M. Hayden, Phys. Rev. Lett. **110**, 137004 (2013).
[6] C. V. Parker, P. Aynajian, E. H. da Silva Neto, A. Pushp, S. Ono, J. Wen, Z. Xu, G. Gu, and A. Yazdani, Nature (London) **468**, 677 (2010).
[7] R. Comin, A. Frano, M. M. Yee, Y. Yoshida, H. Eisaki, E. Schierle, E. Weschke, R. Sutarto, F. He, A. Soumyanarayanan, Yang He, M. Le Tacon, I. S. Elfimov, J. E. Hoffman, G. A. Sawatzky, B. Keimer, and A. Damascelli, Science **343**, 390 (2014).
[8] A. Shekhter, B. J. Ramshaw, R. Liang, W. N. Hardy, D. A. Bonn, F. F. Balakirev, R. D. McDonald, J. B. Betts, S. C. Riggs, and A. Migliori, Nature (London) **498**, 75 (2013).

[9] B. J. Ramshaw, S. E. Sebastian, R. D. McDonald, J. Day, B. Tam, Z. Zhu, J. B. Betts, R. Liang, D. A. Bonn, W. N. Hardy, and N. Harrison, arXiv:1409.3990.
[10] M. Bejas, A. Greco, and H. Yamase, Phys. Rev. B **86**, 224509 (2012).
[11] M. H. Fischer, S. Wu, M. Lawler, A. Paramekanti, and E.-A. Kim, New J. Phys. **16**, 093057 (2014).
[12] Y. Wang and A. V. Chubukov, Phys. Rev. B **90**, 035149 (2014).
[13] V. Oganesyan, S. A. Kivelson, and E. Fradkin, Phys. Rev. B **64**, 195109 (2001).
[14] M. A. Metlitski and S. Sachdev, Phys. Rev. B **82**, 075127 (2010).
[15] M. A. Metlitski and S. Sachdev, New J. Phys. **12**, 105007 (2010).
[16] M. A. Metlitski, D. F. Mross, S. Sachdev, and T. Senthil, arXiv:1403.3694.
[17] L. Nie, G. Tarjus, and S. A. Kivelson, Proc. Nat. Acad. Sci. **111**, 7980 (2014).
[18] V. J. Emery, Phys. Rev. Lett. **58**, 2794 (1987).
[19] C. M. Varma, S. Schmitt-Rink, and E. Abrahams, Solid State Commun. **62**, 681 (1987).
[20] P. B. Littlewood, C. M. Varma, and E. Abrahams, Phys. Rev. Lett. **63**, 2602 (1989).
[21] M. H. Fischer and E.-A. Kim, Phys. Rev. B **84**, 144502 (2011).
[22] S. Bulut, W. A. Atkinson, and A. P. Kampf, Phys. Rev. B **88**, 155132 (2013).
[23] P. B. Littlewood, Phys. Rev. B **42**, 10075 (1990).
[24] S. Graser, T. A. Maier, P. J. Hirschfeld, and D. J. Scalapino, New J. Phys. **11**, 025016 (2009).
[25] In the present phenomenological approach, different bare parameters would be introduced for the spin channel in order to model the spin fluctuations.
[26] S. A. Kivelson, E. Fradkin, and T. H. Geballe, Phys. Rev. B **69**, 144505 (2004).
[27] S. Lederer, Y. Schattner, E. Berg, and S. A. Kivelson, arXiv:1406.1193.